Elementary excitations of a system of one-dimensional chiral fermions with short-range interactions

K. A. Matveev
Materials Science Division, Argonne National Laboratory, Argonne, Illinois 60439, USA

(Received 13 December 2022; revised 3 February 2023; accepted 13 February 2023; published 27 February 2023)

We study general features of the excitation spectrum of a system of one-dimensional chiral spinless fermions with short-range interactions. We show that the nature of the elementary excitations of such a system depends strongly on the nonlinearity of the underlying dispersion of the fermions. In the case of quadratic nonlinearity, the low-momentum excitations are essentially fermionic quasiparticles and quasiholes, whereas the high-momentum ones are classical harmonic waves and solitons. In the case of cubic nonlinearity, the nature of the elementary excitations does not depend on momentum and is determined by the strength of the interactions. At a certain critical value of the interaction strength, the excitation spectrum changes qualitatively, pointing to a dynamic phase transition in the system.

DOI: 10.1103/PhysRevB.107.075438

I. INTRODUCTION

The effect of interactions on the low-energy properties of systems of fermions is strongly enhanced in one dimension. Indeed, in three dimensions, such a system can be described by the Fermi liquid theory [1], in which the elementary excitations are similar to those of the Fermi gas. On the other hand, the low-energy properties of systems of interacting one-dimensional fermions are commonly described in the framework of the Luttinger liquid theory [2,3], in which excitations have bosonic statistics. The best known signature of the Luttinger liquid behavior is the power-law renormalization of the tunneling density of states [4,5].

The issue of the nature of the elementary excitations of the Luttinger liquid is rather subtle. At low energies, many properties of the system, including the tunneling density of states, are described by the Luttinger model, in which the dispersion of the fermions is approximated by two linear chiral branches [6]. In the absence of interactions, the many-body spectrum of this model is highly degenerate. The Hamiltonian of the system can be presented as that of the system of the original fermions or as that of noninteracting bosons. Importantly, the degeneracy is lifted when nontrivial interactions of the fermions are included in the Luttinger model. Typical interactions destroy the picture of free fermionic quasiparticles, whereas the bosons remain noninteracting, albeit with a nonlinear dispersion. Alternatively, the degeneracy of the spectrum can be lifted by including nonlinear corrections to the dispersion of the fermions. This perturbation preserves the picture of free fermionic quasiparticles but generates interactions of bosonic excitations.

In a typical physical realization of one-dimensional fermions, the dispersion is nonlinear, and interactions are not negligible. The nonlinearity is usually quadratic, $\delta\epsilon_p^{(f)} = p^2/2m$, where m is the effective mass of the particles at the Fermi level. On the other hand, for the short-range interactions, the nonlinearity of the bosonic spectrum is cubic, $\delta\epsilon_p^{(b)} = \zeta p^3$. At low energies, corresponding to $p \ll p^* \sim (m\zeta)^{-1}$, the nonlinearity of the fermion dispersion is the dominant perturbation to the Luttinger model at low energies, and the elementary excitations are fermions [7].

The elementary excitations of a system of one-dimensional fermions can be studied in detail [8,9] in the case of strong repulsive interactions, where the crossover momentum p^* is small compared with the Fermi momentum p_F. At low energies, the Hamiltonian of the system splits into two chiral Hamiltonians, which can be reduced [9] to the quantum Korteweg–de Vries (KdV) model [10,11]. At $p \ll p^*$, the system has two branches of elementary excitations near each Fermi point, with dispersions showing quadratic nonlinearities, $\delta\varepsilon_p = \pm p^2/2m^*$. They correspond to the fermionic quasiparticle and quasihole expected from Ref. [7]. The dispersion undergoes a crossover at $p \sim p^*$. At $p \gg p^*$, the quantum KdV Hamiltonian approaches the classical limit. In this regime, one of the excitation branches becomes a boson and has a nonlinear dispersion with $\delta\varepsilon_p \propto p^3$, as expected from the Luttinger model with short-range interactions. The second branch corresponds to the classical KdV soliton; the nonlinearity of its dispersion is $\delta\varepsilon_p \propto p^{5/3}$.

The goal of this paper is to study the spectrum of the elementary excitations of a system of interacting chiral spinless fermions, such as those at the edge of the integer quantum Hall system [12] with occupation fraction $\nu = 1$. We will limit ourselves to the case of short-range interaction and assume that the dispersion of the fermions has either quadratic or cubic nonlinearity. The case of quadratic nonlinearity is relatively straightforward because upon bosonization [2], the Hamiltonian of the system again reduces to that of the quantum KdV model [10,11]. The case of cubic nonlinearity of the fermion dispersion, $\delta\epsilon_p^{(f)} = \gamma p^3$, is qualitatively different. Most importantly, because the dispersion of the bosonic excitations of the Luttinger liquid also has cubic nonlinearity, $\delta\epsilon_p^{(b)} = \zeta p^3$, the relative significance of the dispersion curvature and

interactions does not depend on momentum. The crossover between the regimes of fermionic and bosonic excitations is controlled by the effective interaction strength ζ/γ. Upon bosonization, the Hamiltonian of the system reduces to that of the quantum modified KdV (mKdV) model [11]. Although the latter is known to be integrable [10], no exact results for the dispersion of the elementary excitations are available. We study the excitation spectrum of this model numerically and identify the limits where the elementary excitations are either fermionic quasiparticles and quasiholes or semiclassical phonons and solitons.

The paper is organized as follows. In Sec. II, we study the case of chiral fermions with quadratic dispersion. In particular, we demonstrate that the boundaries of the many-body spectrum coincide with the two branches of the elementary excitations of the system. In Sec. III, we study the case of cubic dispersion. We compute the boundaries of its many-body spectrum numerically and identify the regions where they correspond to the elementary excitations of the system. We summarize and discuss our results in Sec. IV.

II. CHIRAL FERMIONS WITH QUADRATIC DISPERSION

We consider systems of spinless chiral one-dimensional fermions with two-body interactions. In general, the Hamiltonian of such a system has the form:

$$\hat{H} = \sum_p \epsilon_p \vdots c_p^\dagger c_p \vdots + \frac{1}{L} \sum_{\substack{p_1 p_2 \\ q>0}} V(q) c_{p_1+q}^\dagger c_{p_1} c_{p_2}^\dagger c_{p_2+q}. \quad (1)$$

Here, the operator c_p annihilates a fermion in a state with momentum p and energy ϵ_p, and L is the system size. We assume periodic boundary conditions, and thus, p and q are integer multiples of $2\pi\hbar/L$. The notation $\vdots \ldots \vdots$ indicates normal ordering of the fermion operators with respect to the ground state $|0\rangle$, in which all the fermionic states with $p \leqslant 0$ are filled, and those with $p > 0$ are empty.

We are interested in the case of short-range interactions for which the Fourier transform of the interaction potential $V(q)$ is well defined at $q = 0$ along with its second derivative [13]. At sufficiently small q, we then approximate

$$V(q) = V(0) - \eta q^2, \quad (2)$$

where $\eta = -V''(0)/2$. For typical repulsive interactions, $V(0)$ and η are positive.

A single-channel system of chiral fermions has only one Fermi point p_F. As discussed above, even in the vicinity of the Fermi level, it is important to account for the nonlinearity of the dispersion ϵ_p. In this section, we consider the generic case in which the nonlinearity of the dispersion near p_F is quadratic:

$$\epsilon_p = v_F(p - p_F) + \frac{(p - p_F)^2}{2m}. \quad (3)$$

Here, v_F and m are the Fermi velocity and the effective mass. To simplify the treatment of the finite-size effects, we define $p_F = \pi\hbar/L$, which is equidistant from the highest occupied single-particle state $p = 0$ and the lowest unoccupied state $p = 2\pi\hbar/L$ in the many-body ground state $|0\rangle$.

To make further progress, we bosonize the Hamiltonian given by Eqs. (1)–(3) using the standard expression [2] for the fermion annihilation operator at point x,

$$\Psi(x) = \frac{1}{\sqrt{L}} U :e^{i\phi(x)}:. \quad (4)$$

The field $\phi(x)$ is expressed in terms of the bosonic annihilation operators b_l as

$$\phi(x) = 2\pi N \frac{x}{L} - \sum_{l=1}^{\infty} \frac{i}{\sqrt{l}} \left[\exp\left(\frac{i2\pi l x}{L}\right) b_l - \exp\left(-\frac{i2\pi l x}{L}\right) b_l^\dagger \right]. \quad (5)$$

Here, N is the operator of the number of particles measured from that in the ground state $|0\rangle$; the operator U lowers the number of particles by 1, i.e., $[U, N] = U$. The colons in Eq. (4) denote the normal ordering of the bosonic operators b_l and $b_l^\dagger$.

Expressing the fermion operators c_p in the Hamiltonian (1) in terms of the bosonic field $\phi(x)$ with the help of Eq. (4) and substituting Eqs. (2) and (3), we obtain

$$\hat{H} = v(\hat{P} - p_F N) - \frac{\pi^2\hbar^2 N}{6mL^2} + \hat{H}_{\mathrm{KdV}}. \quad (6)$$

Here, $v = v_F + V(0)/2\pi\hbar$, and $\hat{P}$ is the operator of the total momentum of the system:

$$\hat{P} = p_F N + \frac{\hbar}{4\pi} \int_{-L/2}^{L/2} :(\partial_x\phi)^2: dx = \frac{\pi\hbar N(N+1)}{L} + \sum_{l=1}^{\infty} \frac{2\pi\hbar l}{L} b_l^\dagger b_l, \quad (7)$$

measured from that of the ground state $|0\rangle$. The last term in Eq. (6) is given by

$$\hat{H}_{\mathrm{KdV}} = \frac{\hbar^2}{12\pi m} \int_{-L/2}^{L/2} :\left[(\partial_x\phi)^3 - a^*\left(\partial_x^2\phi\right)^2\right]: dx, \quad (8)$$

where $a^* = 3m\eta/2\pi$. Equations (6)–(8) fully account for the effects of changing the particle number in the system. In the following, we limit ourselves to the sector of the Hilbert space corresponding to a fixed number of particles. In this case, without loss of generality, one can set $N = 0$, resulting in

$$\hat{H} = v\hat{P} + \hat{H}_{\mathrm{KdV}}. \quad (9)$$

Since the Hamiltonian (1) conserves momentum, we conclude that $\hat{H}$ and $\hat{H}_{\mathrm{KdV}}$ have common eigenstates and that the corresponding energies of any state with momentum p are related by

$$\varepsilon(p) = vp + \varepsilon_{\mathrm{KdV}}(p), \quad (10)$$

where ε and $\varepsilon_{\mathrm{KdV}}$ are the eigenvalues of the Hamiltonians $\hat{H}$ and $\hat{H}_{\mathrm{KdV}}$, respectively.

In combination with the commutation relation

$$[\phi(x), \partial_y\phi(y)] = -2\pi i\delta(x - y), \quad (11)$$

which follows from Eq. (5), the Hamiltonian (8) defines the quantum KdV problem [10]. It can also be obtained [9] by

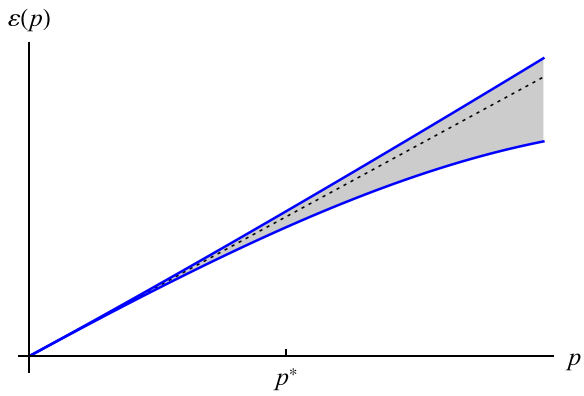

FIG. 1. Dispersions of the two branches of the elementary excitations of the system of interacting chiral fermions with quadratic dispersion. The two solid lines are obtained by combining Eqs. (10) and (12), with the (arbitrarily chosen) velocity value $v = 10p^*/m$. The dotted line shows the linear part of the dispersion relation $\varepsilon(p) = vp$. All the eigenstates of the system are confined to the shaded region between the solid lines.

applying a certain limiting procedure to the bosonized Hamiltonian of either the Lieb-Liniger model [14] or the hyperbolic Calogero-Sutherland model [15,16]. The latter two models have Bethe ansatz solutions, and their elementary excitations are well understood. Using those results, the exact dispersions of the elementary excitations of the quantum KdV model at $L \to \infty$ have been obtained in Ref. [9]:

$$\varepsilon_{\mathrm{KdV}}(p) = \frac{p^{*2}}{2m} e_{\pm}\left(\frac{p}{p^*}\right). \tag{12}$$

Here, $p^* = 3\hbar/2a^*$, which in our notations takes the form:

$$p^* = \frac{\pi\hbar}{m\eta}. \tag{13}$$

The dimensionless functions $e_+(s)$ and $e_-(s)$ correspond to the two branches of the elementary excitations. Their exact analytic expressions (in quadratures) can be found in Ref. [9]; here, we quote their limiting behaviors at large and small s. For the upper branch, we have

$$e_+(s) = \begin{cases} s^2, & s \ll 1, \\ \frac{3}{5}\left(\frac{2\pi}{3}\right)^{2/3} s^{5/3}, & s \gg 1, \end{cases} \tag{14}$$

whereas for the lower one,

$$e_-(s) = \begin{cases} -s^2, & s \ll 1, \\ -s^3, & s \gg 1. \end{cases} \tag{15}$$

The dispersions of the elementary excitations are illustrated in Fig. 1.

The above asymptotic expressions for the energies of the elementary excitations allow for simple physical interpretations. The scaling dimensions of the first and second terms in the Hamiltonian density in Eq. (8) are 3 and 4, respectively. Thus, at small momentum, the second term, which accounts for the interactions of fermions, can be neglected. The remaining term accounts for the quadratic nonlinearity of the dispersion of the fermions. Indeed, at $p \ll p^*$, Eqs. (12), (14), and (15) yield quasiparticle dispersions $\varepsilon_{\mathrm{KdV}} = \pm p^2/2m$, which correspond to the fermionic quasiparticle and quasihole excitations.

At large momentum $p \gg p^*$, the system is in the interaction dominated regime. Substituting Eq. (5) into the second term in Eq. (8), we bring the interaction Hamiltonian to the form:

$$H_{\mathrm{int}} = -\frac{\eta}{2\pi\hbar} \sum_{l=1}^{\infty} p_l^3 b_l^\dagger b_l, \quad p_l = \frac{2\pi\hbar}{L} l. \tag{16}$$

Thus, at large momentum $p \gg p^*$, the nonlinear correction to the energy of the bosonic excitations in the Luttinger liquid approximation scales as $-p^3$, in agreement with the second line of Eq. (15). To obtain the physical interpretation of the other mode, one should restore the small first term in Eq. (8) and derive the equation of motion for the particle density operator $\partial_x\phi/2\pi$. At $p \gg p^*$ and $L \to \infty$, it becomes the classical KdV equation [9]. The latter has two types of solutions. First, there are solutions representing harmonic waves of infinitesimal amplitude, which have cubic dependence of frequency on the wave vector. They are equivalent to the bosonic excitations in Eq. (16). Second, there are soliton solutions of the KdV equation, for which the energy scales as $p^{5/3}$ [9]. They correspond to the second line of Eq. (14).

Let us now discuss the full many-body energy spectrum of the Hamiltonian (8). In the absence of interactions, $\eta = 0$, each of the two simplest many-body states with momentum p contains only a single elementary excitation, a quasiparticle or quasihole, and the corresponding energies are $p^2/2m$ and $-p^2/2m$, respectively. Since any state of the system can be viewed as a combination of particles and holes, and all excitations of a chiral system have positive momenta, the quasiparticle energies $\pm p^2/2m$ are the highest and lowest energies possible at the total momentum p. Because the Bethe ansatz eigenstates at $\eta \neq 0$ can also be classified by occupation numbers of quasiparticles and quasiholes, it is natural to expect [8] that the two branches of elementary excitations in Eq. (12) represent exact boundaries of the many-body spectrum at any interaction strength. This argument applies to many-body states with only a few quasiparticles and quasiholes because their interactions vanish in the limit of infinite system size. A generic state, however, has a finite density of quasiparticles and quasiholes, and the above simple argument does not apply. Nevertheless, we conjecture that Eq. (12) yields the exact boundaries of the excitation spectrum at any η. For the system of interacting chiral fermions defined by Eqs. (1)–(3), this means that the full energy spectrum is confined to the shaded region in Fig. 1.

We now verify the above conjecture by numerical diagonalization of the quantum KdV Hamiltonian (8). In Fig. 2, we plot the upper and lower boundaries of the spectrum normalized by $p^2/2m$. The conjectured values of the boundaries are given by Eq. (12), which upon normalization yields $e_\pm(s)/s^2$, where $s = p/p^*$. We used the analytic expressions for $e_\pm(s)$ obtained in Ref. [9] and plotted $e_\pm(s)/s^2$ as solid lines in Fig. 2. The horizontal axis represents $s = p/p^* = pm\eta/\pi\hbar$, see Eq. (13). In the numerical calculation, we fix the total momentum p and find the highest and lowest eigenvalues of the Hamiltonian (8) for different values of the

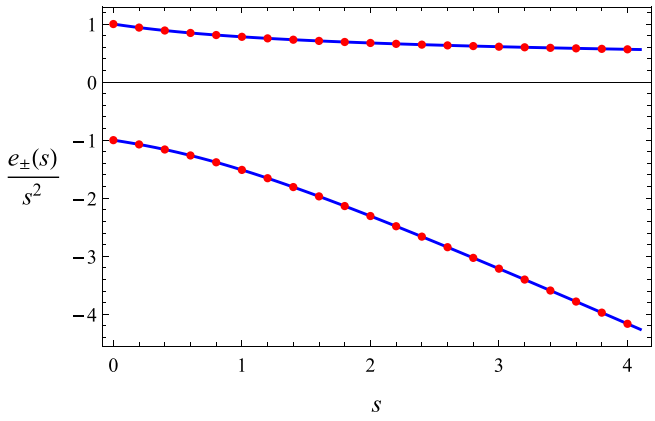

FIG. 2. Comparison of the quasiparticle energies (12) with the boundaries of the spectrum of the Hamiltonian (8). The horizontal axis s is the momentum in units of p^* given by Eq. (13). The solid lines are the energies (12) divided by $p^2/2m$. The dots represent the numerically computed boundaries of the energy spectrum of the Hamiltonian (8) extrapolated to infinite system size.

interaction strength η. The eigenvalues are then divided by $p^2/2m$, and the results are extrapolated numerically to the limit of infinite system size [17]. The resulting boundaries of the spectrum are shown by dots in Fig. 2. They are in excellent agreement with the conjectured values.

To summarize the results of this section, we have studied the elementary excitations of the system of interacting chiral spinless fermions described by Eqs. (1)–(3). Upon bosonization, the Hamiltonian reduces to that of the quantum KdV model, see Eq. (8). At low momentum, the excitations are the fermionic quasiparticle and quasihole. At high momentum, they become the KdV soliton and the harmonic wave. The energies are given by Eqs. (10) and (12), where the exact expressions for the functions $e_\pm(s)$ can be found in Ref. [9]. The two quasiparticle branches are shown in Fig. 1. They represent the exact boundaries of the many-body spectrum of the system.

III. CHIRAL FERMIONS WITH CUBIC DISPERSION

A. Hamiltonian

We now turn to the special regime of the interacting system of spinless chiral fermions, in which the Fermi momentum p_F coincides with an inflection point of the dispersion ϵ_p. In this case, the effective mass m is infinite, and ϵ_p has a cubic nonlinearity near the Fermi point:

$$\epsilon_p = v_F(p - p_F) + \gamma(p - p_F)^3. \tag{17}$$

In the following, we assume $\gamma > 0$. The results for negative γ can be obtained by trivial symmetry transformations.

Next, we apply the bosonization transformation (4) to bring the Hamiltonian given by Eqs. (1), (2), and (17) to the form:

$$\hat{H} = \left(v - \frac{\pi^2\hbar^2\gamma}{L^2}\right)(\hat{P} - p_F N) + \hat{H}_{\rm mKdV}. \tag{18}$$

Here again, $v = v_F + V(0)/2\pi\hbar$, the operator of the total momentum is defined by Eq. (7), and we again chose the Fermi momentum $p_F = \pi\hbar/L$. The last term is given by

$$H_{\rm mKdV} = \frac{\hbar^3\gamma}{8\pi}\int_{-L/2}^{L/2} :\left[(\partial_x\phi)^4 + (1-2\chi)\left(\partial_x^2\phi\right)^2\right]: dx, \tag{19}$$

where $\chi = \eta/2\pi\hbar\gamma$. In combination with the commutation relation (11), the Hamiltonian (19) defines the quantum mKdV problem [10]. In the limit of infinite system size, the relation between the quantum mKdV Hamiltonian and that of chiral fermions was discussed in Ref. [11].

Unlike the case of quadratic nonlinearity (3), the Hamiltonian given by Eqs. (1), (2), and (17) possesses particle-hole symmetry, i.e., it retains its form under the transformation

$$c_{p_F+q} \to c^\dagger_{p_F-q}, \quad \Psi(x) \to \Psi^\dagger(x)\exp\left(\frac{i2\pi x}{L}\right). \tag{20}$$

In the bosonized form, this property is expressed as

$$U \to U^\dagger, \quad \phi(x) \to -\phi(x), \quad b_l \to -b_l, \quad N \to -N, \tag{21}$$

see Eqs. (4) and (5).

Since the Hamiltonian $\hat{H}$ conserves the total momentum $\hat{P}$, it follows from Eq. (18) that it has the same eigenstates at $H_{\rm mKdV}$. In the sector of the Hilbert space with the number of particles equal to that in the ground state $|0\rangle$, one should set $N = 0$. In this case, the eigenvalues of the two Hamiltonians are related by

$$\varepsilon(p) = vp + \varepsilon_{\rm mKdV}(p), \tag{22}$$

where we omitted the finite-size correction to the velocity v in Eq. (18).

B. Boundaries of the energy spectrum

Our next goal is to study the boundaries of the energy spectrum of the quantum mKdV Hamiltonian (19) in the limit of infinite system size, $L \to \infty$. We start with the case of free fermions, corresponding to $\chi = 0$. In this case, the system supports two types of elementary excitations: quasiparticles and quasiholes. The particle-hole symmetry of the Hamiltonian (19) ensures that the quasiparticles and quasiholes with momentum p have the same energy γp^3. The latter is the highest energy of any eigenstate of the Hamiltonian (19) with momentum p at $\chi = 0$. The lowest possible energy at $L \to \infty$ is 0. To obtain an eigenstate with energy near this lower boundary, the total momentum p should be divided among many particle-hole pairs, each carrying a very small fraction of the total momentum.

In addition to the case of vanishing interactions, $\chi = 0$, the Hamiltonian (19) can be easily treated analytically in the limits of strong repulsive or attractive interactions, $\chi \to \pm\infty$. In this case, the second term in Eq. (19) dominates. Using Eq. (5), the latter can be written in terms of the bosonic operators b_l:

$$H_{\rm mKdV} \simeq \gamma\left(\frac{1}{2} - \chi\right)\sum_{l=1}^{\infty} p_l^3 b_l^\dagger b_l, \quad p_l = \frac{2\pi\hbar}{L}l, \tag{23}$$

cf. Eq. (16). A system described by the Hamiltonian (23) has bosonic elementary excitations with energies $\gamma(\frac{1}{2} - \chi)p^3$. This expression also yields the lower (upper) boundary of the full energy spectrum at positive (negative) $\chi - \frac{1}{2}$. The other boundary of the spectrum at $L \to \infty$ is at zero energy. It corresponds to the state in which the total momentum p of

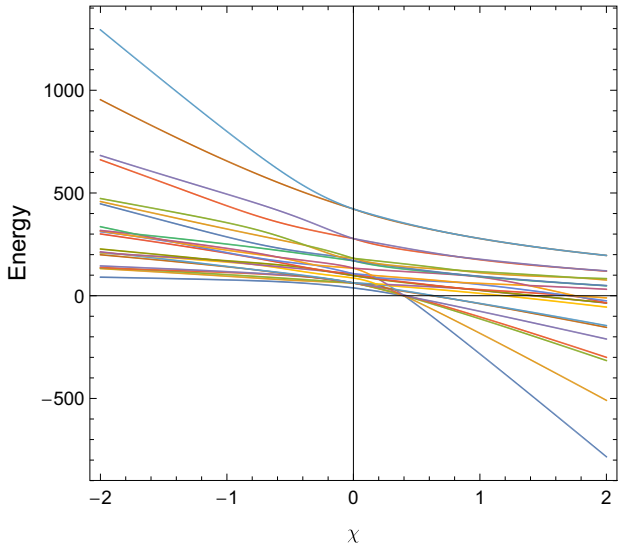

FIG. 3. The energy spectrum of the Hamiltonian (19) for the total momentum $P = 8$ in units of $2\pi\hbar/L$. The units are chosen so that $\gamma = \hbar = 1$ and $L = 2\pi$. The solid lines show the positions of the 22 energy levels for each value of the parameter χ. (We have subtracted $P/4 = 2$ from all eigenvalues to account for the term $-(\pi^2\hbar^2\gamma/L^2)\hat{P}$ in Eq. (18) [17].) At $\chi = 0$, the two highest energy states are degenerate, corresponding to the single quasiparticle and quasihole with energies $(P - \frac{1}{2})^3 + \frac{1}{8} = 422$.

the system is distributed among an infinite number of bosons with infinitesimal momentum.

We showed so far that, at $\chi = 0$ and $\chi \to \pm\infty$, the eigenstates of the Hamiltonian (19) with a given momentum p are confined to regions with the boundaries that scale as p^3. Because both contributions to the Hamiltonian density in Eq. (19) have scaling dimension 4, this observation holds for any value of χ. Furthermore, the form of the Hamiltonian (19) ensures that, for any given χ, all the energies are proportional to γ. Thus, the upper and lower boundaries of the spectrum can be presented in the form:

$$\varepsilon_{\mathrm{mKdV}}(p) = \alpha_{\pm}(\chi)\gamma p^3. \tag{24}$$

The above results for $\chi = 0$ and $\chi \to \pm\infty$ can be summarized as

$$\alpha_+(\chi) = \begin{cases} \frac{1}{2} - \chi, & \chi \to -\infty, \\ 1, & \chi = 0, \\ 0, & \chi \to +\infty, \end{cases} \tag{25}$$

and

$$\alpha_-(\chi) = \begin{cases} 0, & \chi \to -\infty, \\ 0, & \chi = 0, \\ \frac{1}{2} - \chi, & \chi \to +\infty. \end{cases} \tag{26}$$

The Hamiltonian (19) can be diagonalized numerically for moderate values of the total momentum p. The results for the full energy spectrum in the case of $p = 8 \times 2\pi\hbar/L$ are shown in Fig. 3. The functions $\alpha_+(\chi)$ and $\alpha_-(\chi)$ can then be computed by extrapolating the energies of the highest and lowest levels to the limit $L \to \infty$ at fixed p, see Fig. 4.

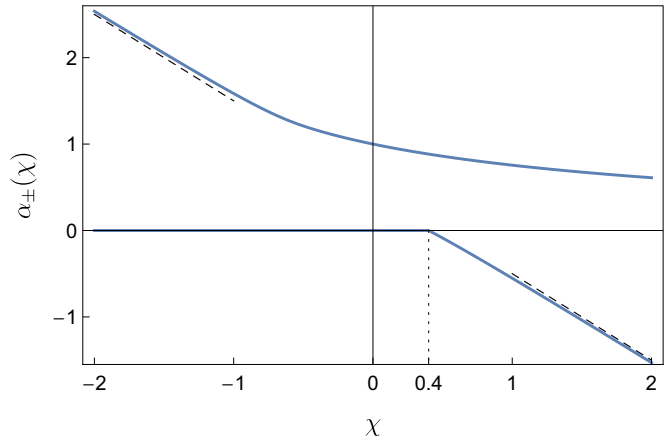

FIG. 4. The functions $\alpha_+(\chi)$ and $\alpha_-(\chi)$ evaluated numerically [17] are shown by the top and bottom solid lines, respectively. The dashed lines represent the result $\frac{1}{2} - \chi$ for the bosonic excitation branch, Eq. (23), which controls one of the boundaries at large $|\chi|$, see Eqs. (25) and (26). Note that, at $\chi < \chi_c \approx 0.4$, we have $\alpha_-(\chi) = 0$.

The function $\alpha_-(\chi)$ shows two distinct types of behavior. When the dimensionless interaction parameter is large and positive ($\chi \to +\infty$), α_- scales as $\frac{1}{2} - \chi$, in agreement with Eq. (26). As we discussed, the corresponding lowest energy state of the system at a given value p of the total momentum has a single bosonic excitation with momentum p. As χ is lowered, $\alpha_-(\chi)$ increases until it reaches zero at $\chi = \chi_c \approx 0.4$. At $\chi < \chi_c$, the lowest possible energy of the system remains zero. As we saw earlier, this is indeed the case for $\chi = 0$ and $\chi \to -\infty$, see Eq. (26). The lowest energy state in these cases corresponded to the total momentum p being distributed among an infinite number of elementary excitations with infinitesimal momentum. The numerical results of Fig. 4 imply that this is the case for all $\chi < \chi_c$.

The behavior of the function $\alpha_+(\chi)$, which describes the upper boundary of the spectrum, is qualitatively different. It scales as $\frac{1}{2} - \chi$ at large negative χ, which corresponds to the energy of the system with a single bosonic excitation, see Eqs. (23) and (25). It decreases gradually as χ increases. At $\chi = 0$, it reaches the value $\alpha_+(0) = 1$, corresponding to a state of free chiral Fermi gas with a single quasiparticle or quasihole excitation. It continues to decrease at positive χ and gradually approaches zero at $\chi \to +\infty$, see Eq. (25). The nature of the highest energy state at $\chi \gg 1$ is not self-evident, but our discussion in Sec. II suggests that it may be related to the classical soliton solutions of the modified KdV equation.

C. Solitons

To study the classical limit of the Hamiltonian (19), we use the commutation relation (11) to write the equation of motion for the operator $\phi(x, t)$:

$$\frac{1}{\hbar^2\gamma}\partial_t\phi = -(\partial_x\phi)^3 + \left(\frac{1}{2} - \chi\right)\partial_x^3\phi. \tag{27}$$

In the classical limit, $\phi(x, t)$ is no longer an operator, and thus, we ignored normal ordering. The conditions under which this approximation is applicable will be established later.

Next, we introduce $\tau = \hbar^2\gamma t$, differentiate Eq. (27) with respect to x, and obtain a partial differential equation for the function

$$u(x,\tau) = \partial_x\phi(x,\tau) \tag{28}$$

in the form

$$\partial_\tau u + 3u^2\partial_x u + \tilde{\chi}\,\partial_x^3 u = 0, \quad \tilde{\chi} = \chi - \tfrac{1}{2}. \tag{29}$$

This is the well-known classical modified KdV equation [18]. At $\tilde{\chi} > 0$, it has two soliton solutions:

$$u(x,\tau) = \pm\frac{\sqrt{2c}}{\cosh\left(\sqrt{\frac{c}{\tilde{\chi}}}(x - c\tau)\right)}, \tag{30}$$

where $c > 0$. No soliton solutions exist for $\tilde{\chi} < 0$.

We are now in a position to obtain the condition of applicability of the classical approximation used in deriving Eq. (27). Equation (30) yields the order of magnitude estimate $u \sim \sqrt{c}$. Given that the spatial scale of the soliton solution is $\sqrt{\tilde{\chi}/c}$, Eq. (28) yields $\phi \sim u\sqrt{\tilde{\chi}/c} \sim \sqrt{\tilde{\chi}}$. According to Eq. (11), the commutator of $\phi(x)$ and $\phi(y)$ is of order unity. Classical approximation assumes that it is small compared with $\phi(x)\phi(y) \sim \tilde{\chi}$. Thus, the classical results are applicable at $|\tilde{\chi}| \gg 1$ or, equivalently, $|\chi| \gg 1$.

Integrating the standard bosonization expression for the particle density $n(x) = \partial_x\phi/2\pi = u/2\pi$ with respect to x, we find the total number of fermions carried by a single soliton:

$$N_s = \pm\sqrt{\frac{\tilde{\chi}}{2}}. \tag{31}$$

Thus, at $\tilde{\chi} \gg 1$, when the classical mKdV theory applies to the chiral Fermi system with cubic dispersion, the soliton carries a large number of particles, $|N_s| \gg 1$.

Next, we substitute Eq. (28) into Eqs. (7) and (19) to obtain the expressions for the momentum and energy of the soliton (30) in the limit $L \to \infty$. This yields

$$p = \frac{\hbar}{4\pi}\int_{-\infty}^{\infty} u^2 dx = \frac{\hbar}{\pi}\sqrt{c\tilde{\chi}},$$

$$E = \frac{\hbar^3\gamma}{8\pi}\int_{-\infty}^{\infty}[u^4 + (1-2\chi)u'^2]dx = \frac{\hbar^3\gamma}{3\pi}\sqrt{c^3\tilde{\chi}}.$$

These expressions give the dispersion relation for the soliton in the form:

$$E(p) = \frac{\pi^2}{3\tilde{\chi}}\gamma p^3. \tag{32}$$

As expected, the energy scales with the third power of momentum.

Similar to the case of a system of chiral fermions with quadratic dispersion discussed in Sec. II, soliton behaves as an elementary excitation of the system. Although states involving many solitons are possible, the convex shape of the dispersion relation (32) suggests that the state with one soliton has the largest energy at a given momentum. This implies the following behavior of $\alpha_+(\chi)$ at large χ:

$$\alpha_+(\chi) \simeq \frac{2\pi^2}{3(2\chi - 1)}, \quad \chi \gg 1, \tag{33}$$

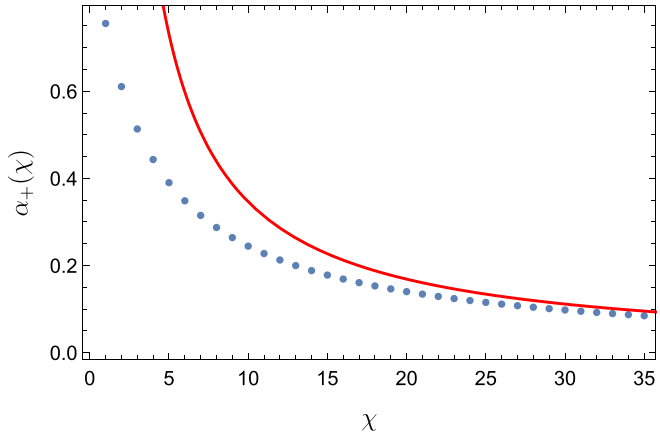

FIG. 5. Comparison of the numerically computed $\alpha_+(\chi)$ for $\chi = 1, 2, \ldots, 35$ (dots) with the asymptotic behavior (33) shown by the solid line.

where we used Eqs. (24) and (32) and the definition of $\tilde{\chi}$ from Eq. (29). The asymptotic behavior (33) is consistent with our earlier expectation of the limiting value at $\chi \to +\infty$ in Eq. (25). It can also be compared with the numerical results for $\alpha_+(\chi)$, but this requires extending the computation to much larger values of χ than those shown in Fig. 4. Such a comparison shows good agreement at $\chi \gtrsim 20$, see Fig. 5.

D. Interpretation in terms of elementary excitations

In Sec. II, we discussed the dispersions (12) of the elementary excitations of the quantum KdV model (8) and demonstrated that they also define the boundaries of the many-body spectrum of the system at $L \to \infty$. The elementary excitations were studied in Ref. [9] with the help of the Bethe ansatz solutions of the Lieb-Liniger [14] and hyperbolic Calogero-Sutherland [16] models, which reduce to the quantum KdV model under proper limiting procedures. Unfortunately, no mapping of this kind is known for the quantum mKdV model (19). Furthermore, even though this model is believed to be integrable [10], a Bethe ansatz solution is not currently available. Thus, we so far focused on obtaining the boundaries of the many-body spectrum of the Hamiltonian (19) at $L \to \infty$. We now discuss to what extent they can be interpreted as elementary excitations of the system.

We start with the case of noninteracting fermions. If the dispersion is quadratic, the quasiparticle and quasihole with momentum p have energies $p^2/2m$ and $-p^2/2m$, respectively. These values are the highest and lowest possible energies of any eigenstate with the total momentum p. In contrast, if the dispersion is cubic, both the quasiparticle and quasihole have the same energy γp^3, which can be interpreted as a consequence of the particle-hole symmetry of the Hamiltonian. Due to the convexity of the dispersion γp^3, it also yields the upper boundary of the many-body spectrum. The lowest energy state can be constructed by distributing the total momentum p among a large number of quasiparticles and quasiholes [17]. At $L \to \infty$, the corresponding energy is 0.

A similar interpretation of the boundaries of the spectrum applies in the limit of strong attractive interactions, $\chi \to$

$-\infty$. In this case, to leading order, the Hamiltonian takes the form (23). The highest energy state has a single bosonic excitation:

$$\psi_o(p) = b_p^\dagger|0\rangle, \quad E_o(p) = \gamma\left(\tfrac{1}{2} - \chi\right)p^3. \tag{34}$$

Here, the subscript o indicates that the state contains an odd number of bosonic excitations, which means that it is odd with respect to the particle-hole symmetry, see Eq. (21). The highest energy even state is

$$\psi_e(p) = b_{p-p_1}^\dagger b_{p_1}^\dagger|0\rangle, \quad E_e(p) \simeq E_o(p)\left(1 - \frac{3p_1}{p}\right), \tag{35}$$

where $p_1 = 2\pi\hbar/L$. In the limit of infinite system size, the respective energies are equal, $E_o(p) = E_e(p)$. The lowest energy eigenstates of the Hamiltonian (23) with large negative χ in the two parity sectors are

$$(b_{p_1}^\dagger)^{\frac{p}{p_1}}|0\rangle, \quad (b_{p_1}^\dagger)^{\frac{p}{p_1}-2}b_{2p_1}^\dagger|0\rangle. \tag{36}$$

The corresponding energies vanish at $L \to \infty$.

In the above examples, the system has two branches of elementary excitations, which correspond to states that are even and odd with respect to particle-hole symmetry, with energies that become identical at $L \to \infty$. The dispersion $\varepsilon(p)$ of the excitations defines the upper boundary of the excitation spectrum of the quantum mKdV Hamiltonian (19), while the lower boundary is at zero energy. Our results for the boundaries of the energy spectrum at $L \to \infty$ given by Eq. (24) and Fig. 4 suggest that the same picture applies at all $\chi < \chi_c \approx 0.4$. Then the dispersion of the elementary excitations is

$$\varepsilon_{\text{mKdV}}^{+}(p) = \alpha_+(\chi)\gamma p^3. \tag{37}$$

The function $\alpha_+(\chi)$ shown by the upper line in Fig. 4 continues into the region $\chi > \chi_c$, suggesting that the excitation branch with dispersion given by Eq. (37) exists at all interaction strengths. On the other hand, the lower boundary of the spectrum corresponds to negative energies at $\chi > \chi_c$. Furthermore, at $\chi \to \infty$, the approximation (23) applies again. The dispersion associated with the two excitation branches (34) and (35) is now concave and thus describes the lower boundary of the energy spectrum. This suggests that, in addition to the excitation branch (37), there is another one, with dispersion

$$\varepsilon_{\text{mKdV}}^{-}(p) = \alpha_-(\chi)\gamma p^3, \quad \chi > \chi_c. \tag{38}$$

Our results for the boundaries of the spectrum do not preclude the possibility that this branch continues into the region $\chi < \chi_c$. Indeed, a mode with energy $\alpha^*\gamma p^3$ would not affect the boundaries of the many-body spectrum at $\chi < \chi_c$ if $0 < \alpha^* < \alpha_+$. We note, however, that at $\chi = 0$, when the model describes free fermions, quasiparticles and quasiholes are the only types of excitations present, and their dispersion is given by Eq. (37). Thus, the branch (38) must terminate at some value of χ between 0 and χ_c. Some numerical evidence supporting this scenario is obtained by studying overlaps of the single boson state with all the eigenstates of the Hamiltonian with $0 < \chi < \chi_c$ [17].

IV. DISCUSSION OF THE RESULTS

In Sec. II, we studied the elementary excitations and the boundaries of the many-body spectrum of the system of spinless chiral fermions with short-range interactions. Upon bosonization, the problem reduces to the quantum KdV model (8), for which exact results for the excitation spectrum are available [9]. We concluded that, at $p \ll p^*$, the excitations are essentially the quasihole and quasiparticle of the free Fermi gas, while at $p \gg p^*$, they are the bosonic density wave and the KdV soliton. Using the definition (13) of p^*, this can be alternatively interpreted as crossover between the regimes of weak and strong interactions. Given the curvature of the dispersions of the two excitation branches, Fig. 1, it is natural to expect that they would coincide with the lowest and highest energies of many-body states with total momentum p. This conjecture is confirmed by our numerical calculations.

Our main focus was on the study of the system of interacting spinless chiral fermions with cubic dispersion, Sec. III. Bosonization reduces this problem to the quantum mKdV model (19). The scaling properties of this model dictate that the energy scales associated with it must be proportional to p^3. This applies, in particular, to the boundaries of the many-body spectrum, which we obtained numerically, see Eq. (24) and Fig. 4. Unlike the case of quadratic dispersion studied in Sec. II, we found two distinct regimes of interaction strength. At $\chi > \chi_c$, the system behaves like the quantum KdV model (8) in that both boundaries of the many-body spectrum can be viewed as states with one elementary excitation. The excitation belongs to one of two branches, with dispersions given by Eqs. (37) and (38). This analogy fails at $\chi < \chi_c$, where only the upper boundary of the excitation spectrum behaves as an elementary excitation; its dispersion is given by Eq. (37). At $\chi = 0$ and $\chi \to -\infty$, the lower boundary corresponds to states with an infinite number of excitations, each carrying infinitesimal momentum. It is natural to apply the same interpretation to the lower boundary of the spectrum at all $\chi < \chi_c$.

The existence of two qualitatively different regimes depending on the interaction strength could have been anticipated by considering the limit of strong interactions, $|\chi| \to \infty$. In this limit, the system is described by the classical mKdV equation (29). The latter has harmonic wave solutions with infinitesimal amplitude, for which the nonlinear term in Eq. (29) can be neglected. They correspond to the bosonic excitations giving the upper (lower) boundary of the spectrum at $\chi \to -\infty$ ($\chi \to +\infty$). In addition, at $\tilde{\chi} > 0$, the mKdV equation (29) has soliton solutions. In analogy with the quantum KdV model (8), the soliton gives the upper boundary of the excitation spectrum, see Sec. III C. In contrast, no soliton solutions exist at $\tilde{\chi} < 0$, resulting in the qualitatively different behavior of the lower boundary of the spectrum at $\chi \to -\infty$.

The energy eigenvalues of the original model of chiral fermions with cubic dispersion are related to those of the quantum mKdV model by Eq. (22). Our results are illustrated in Fig. 6, where the boundaries of the energy spectrum are shown in the two regimes, $\chi < \chi_c$ and $\chi > \chi_c$. The behavior of the energy spectrum in the latter regime is similar to that for fermions with quadratic dispersion, see Fig. 1.

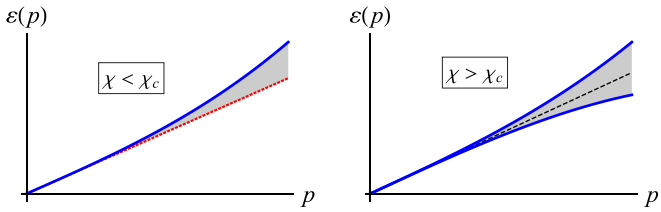

FIG. 6. Boundaries of the many-body spectrum of the system of chiral fermions with cubic dispersion and short-range interactions. For all χ, the upper boundary is given by $\varepsilon = vp + \varepsilon^{+}_{\mathrm{mKdV}}(p)$, see Eq. (37). At $\chi < \chi_c$, the lower boundary of the spectrum is the straight dotted line $\varepsilon = vp$, while at $\chi > \chi_c$, it is given by $\varepsilon = vp + \varepsilon^{-}_{\mathrm{mKdV}}(p)$, see Eq. (38).

Let us now briefly discuss the expected behavior of the dynamic response functions of the system, which include the spectral function $A(p, \epsilon)$ and the dynamic structure factor $S(p, \epsilon)$. The shaded regions in Figs. 1 and 6 correspond to the possible energies of the system at a given momentum. The response functions must vanish outside these regions. In nonchiral systems, the behavior of $A(p, \epsilon)$ and $S(p, \epsilon)$ near the edge of support was studied phenomenologically using the mobile impurity model [19,20]. This approach should be applicable near the boundaries of the spectrum of chiral fermions with quadratic dispersion, which allow for the interpretation as states with one elementary excitation. It should also apply to the boundaries shown by solid lines in Fig. 6 for the case of fermions with cubic dispersion. In the nonchiral case, both $A(p, \epsilon)$ and $S(p, \epsilon)$ were predicted to scale as a power of the distance from the boundary [19,20]. We expect an analogous power-law scaling in the chiral case.

The lower boundary of the spectrum at $\chi < \chi_c$, shown by the dotted line in Fig. 6, has a different nature. The states near this boundary involve a large number of excitations with very small momenta. A similar problem has been studied in the case of phonons in liquid helium, where the exponential suppression of the response was found [21]. In the case of one-dimensional systems with linear spectrum, equivalent to the limit $\chi \to -\infty$ of our model, the exponential suppression of the spectral function was found in Ref. [22]. Furthermore, in the case of weakly interacting fermions, $|\chi| \ll 1$, the overlap of a low-energy state involving a large number of particle-hole pairs with that involving a single pair occurs in a high order of the perturbation theory. As a result, the response functions must again be exponentially small near the boundary. We therefore expect exponential suppression of the dynamic response functions near the lower boundary of the spectrum at $\chi < \chi_c$. Our numerical treatment of the Hamiltonian (19) supports this conclusion [17].

The qualitative change of the energy spectrum at the interaction strength $\chi = \chi_c$ can be interpreted as a phase transition in the system. Interestingly, this phase transition is purely dynamic, in that it appears only in the dynamic response functions of the system. Indeed, due to the chiral nature of the problem, the ground state $|0\rangle$, which corresponds to the filled Fermi surface, does not depend on the interaction strength. Thus, the static properties of the system are not affected by the interactions. Alternatively, one can consider the behavior of the system at a fixed value p of the total momentum. In this case, the ground state energy as a function of the interaction strength χ shows nonanalytic behavior at $\chi = \chi_c$, which can be interpreted as a quantum phase transition. A similar nonanalytic behavior of the boundary of the energy spectrum at a fixed momentum was recently found in the system of chiral fermions with quadratic spectrum and Coulomb interactions [23]. Finally, we note that, in our numerical data represented in Fig. 4, we have not been able to find a deviation of χ_c from 0.4, i.e., we expect that the exact value is $\chi_c = \frac{2}{5}$.

ACKNOWLEDGMENTS

The author is grateful to A. Furusaki, I. Martin, M. R. Norman, and M. Pustilnik for helpful discussions. This work was supported by the U.S. Department of Energy, Office of Science, Basic Energy Sciences, Materials Sciences and Engineering Division.

[1] E. M. Lifshitz and L. P. Pitaevskii, *Statistical Physics, Part 2* (Butterworth-Heinemann, Oxford, 1980).
[2] F. D. M. Haldane, 'Luttinger liquid theory' of one-dimensional quantum fluids. I. Properties of the Luttinger model and their extension to the general 1D interacting spinless Fermi gas, J. Phys. C: Solid State Phys. **14**, 2585 (1981).
[3] T. Giamarchi, *Quantum Physics in One Dimension* (Clarendon, Oxford, 2004).
[4] C. L. Kane and M. P. A. Fisher, Transmission through barriers and resonant tunneling in an interacting one-dimensional electron gas, Phys. Rev. B **46**, 15233 (1992).
[5] A. Furusaki and N. Nagaosa, Single-barrier problem and Anderson localization in a one-dimensional interacting electron system, Phys. Rev. B **47**, 4631 (1993).
[6] J. M. Luttinger, An exactly soluble model of a many-fermion system, J. Math. Phys. **4**, 1154 (1963).
[7] A. V. Rozhkov, Fermionic quasiparticle representation of Tomonaga-Luttinger Hamiltonian, Eur. Phys. J. B **47**, 193 (2005).
[8] M. Pustilnik and K. A. Matveev, Solitons in a one-dimensional Wigner crystal, Phys. Rev. B **91**, 165416 (2015).
[9] M. Pustilnik and K. A. Matveev, Fate of classical solitons in one-dimensional quantum systems, Phys. Rev. B **92**, 195146 (2015).
[10] R. Sasaki and I. Yamanaka, Field theoretical construction of an infinite set of quantum commuting operators related with soliton equations, Commun. Math. Phys. **108**, 691 (1987).
[11] A. K. Pogrebkov, Boson-fermion correspondence and quantum integrable and dispersionless models, Russ. Math. Surv. **58**, 1003 (2003).
[12] B. I. Halperin, Quantized Hall conductance, current-carrying edge states, and the existence of extended states in a

two-dimensional disordered potential, Phys. Rev. B **25**, 2185 (1982).

[13] For an interaction potential that falls off as a power of the distance x between the fermions, $U(x) \propto 1/|x|^{\lambda}$ at $|x| \to \infty$, this condition requires $\lambda > 3$.

[14] E. H. Lieb and W. Liniger, Exact analysis of an interacting Bose gas. I. The general solution and the ground state, Phys. Rev. **130**, 1605 (1963).

[15] B. Sutherland, A brief history of the quantum soliton with new results on the quantization of the Toda lattice, Rocky Mountain J. Math. **8**, 413 (1978).

[16] B. Sutherland, *Beautiful Models: 70 Years of Exactly Solved Quantum Many-body Problems* (World Scientific, Singapore, 2004).

[17] See Supplemental Material at http://link.aps.org/supplemental/10.1103/PhysRevB.107.075438 for the details.

[18] G. L. Lamb, *Elements of Soliton Theory* (Wiley, New York, 1980).

[19] A. Imambekov and L. I. Glazman, Phenomenology of One-Dimensional Quantum Liquids Beyond the Low-Energy Limit, Phys. Rev. Lett. **102**, 126405 (2009).

[20] A. Imambekov, T. L. Schmidt, and L. I. Glazman, One-dimensional quantum liquids: Beyond the Luttinger liquid paradigm, Rev. Mod. Phys. **84**, 1253 (2012).

[21] S. V. Iordanskii and L. P. Pitaevskii, Properties of the endpoint of a multiphonon spectrum, ZhETF Pisma Redaktsiiu **27**, 658 (1978) [JETP Lett. **27**, 621 (1978)].

[22] K. A. Matveev, Spectral Function of the Chiral One-Dimensional Fermi Liquid in the Regime of Strong Interactions, Phys. Rev. Lett. **128**, 176802 (2022).

[23] I. Martin and K. A. Matveev, Scar states in a system of interacting chiral fermions, Phys. Rev. B **105**, 045119 (2022).